

A study of abrasive waterjet cutting of metallic coated sheet steels

Author:

Wang, Jun

Publication details:

International Journal of Machine Tools and Manufacture

v. 39

Chapter No. 6

pp. 855-870

Publication Date:

1999

License:

<https://creativecommons.org/licenses/by-nc-nd/3.0/au/>

Link to license to see what you are allowed to do with this resource.

Downloaded from <http://hdl.handle.net/1959.4/11060> in <https://unsworks.unsw.edu.au> on 2024-03-28

A study of abrasive waterjet cutting of metallic coated sheet steels

J. WANG[†]

Abstract – A study of Abrasive Waterjet (AWJ) cutting of metallic coated sheet steels is presented based on a statistically designed experiment. It shows that AWJ cutting is a viable technology for processing metallic coated sheet steels with good productivity and kerf quality. A scanning electron microscopy analysis indicates that micromachining and plastic deformation are the dominant cutting phenomena in sheet steel processing. Plausible trends and relationships between kerf characteristics and process parameters are discussed. It is found that an optimum water pressure together with small standoff distance between the nozzle and workpiece may be used, while the traverse speed should be selected as high as possible for through cuts in order to increase the cutting rate. Empirical models for kerf geometry and quality are finally established for the prediction and optimization of AWJ cutting performance.

1. INTRODUCTION

While metallic coated sheet metals have found extensive applications, the processing of such materials has primarily relied on conventional punching and blanking. These methods may be claimed to be justified and effective in mass production, however, manufacturing industry is getting more time conscious and the requirement for prototype samples and small production batch is increasing. To cope with this trend, laser cutting technology has been employed. Unfortunately, metallic coated sheet metals exhibit an anomalous behaviour when subjected to the laser light due to the high reflectivity and thermal conductivity of the coatings [1]. As a consequence, both productivity and workpiece quality are affected.

By contrast, Abrasive Waterjet (AWJ) cutting technology, which is claimed to have the distinct advantages of no thermal distortion, high machining versatility, high flexibility and small cutting forces [2], offers potential for the processing of metallic coated sheet steels. A considerable amount of work has been conducted in recent years to study the mechanism of AWJ cutting and to develop kerf geometry and surface roughness models for process control and optimization [3-15]. These have involved the processing of ductile [4-8] and brittle materials [9-11], leathers, woods and rubbers [12], as well as composites and plastics [16,17]. It is interesting to note, however, that very little has been reported on the AWJ cutting of thin sheet steels [18] and there is little knowledge of the cutting performance in AWJ machining of metallic coated sheet metals.

In this paper, a study of Abrasive Waterjet cutting of metallic coated sheet steels is presented which examines the cutting performance as assessed by the various kerf characteristic measures (i.e. kerf shape and quality) and the effect of process parameters on the kerf characteristics using a statistically designed experiment. Visual examination and scanning electron microscopy (SEM) analysis is employed to study the topography of the cut surfaces and to develop a further understanding of the mechanism of sheet metal processing under abrasive waterjets. Statistical analysis of the trends and relationships between the kerf characteristics and the process parameters, as well as the selection of the process parameters for cutting the material under investigation, are also discussed together with the established empirical equations.

[†] School of Mechanical, Manufacturing and Medical Engineering, Queensland University of Technology (QUT), GPO Box 2434, Brisbane, Queensland 4001, Australia. (Email: j.wang@qut.edu.au).

2. BACKGROUND

AWJ cutting technology uses a jet of high pressure and velocity water and abrasive slurry to cut the target material by means of erosion. In early investigations, it has been found [4,9] that three cutting zones exist in the processing of ductile and brittle materials under abrasive waterjets, namely, the primary cutting zone at shallow angles of attack, the secondary cutting zone at large angles of attack, and the jet upward deflection zone. The attack angle is defined as the angle between the initial jet direction and the particle cutting direction. Based on the proposal by Bitter [19] and Finnie [20] for particle erosion of materials, Hashish [3] claimed that the cutting mechanism in the first two zones could be considered as cutting wear and deformation wear, respectively. It is proposed that the cutting wear mode is characterized by ploughing and cutting deformation, where ploughing occurs at large negative rake angle by the abrasives while cutting deformation occurs when the particles cut the material at positive rake angles. The wear process is similar to that in conventional grinding process, however, it is very difficult to describe since the particles may have linear velocity as well as angular velocity. The surface generated by the cutting wear is generally of good finish and can be assessed by a surface roughness measure, such as centre-line average.

In the steady cyclic cutting stage, the particles will change the attack angle between the initial jet and cutting directions from shallow to large and have reduced kinetic energy due to such phenomena as particle deflection, reduction in impact velocity and particle fragmentation. Under this condition, material is removed by cutting as well as deformation (or the so-called deformation wear) processes where the particles push the material into a plastic state until it is removed. Chen *et al.* [9] show that as the jet further penetrates into the workpiece, deformation is the dominant mechanism. This is associated with striations formed at the lower portion of the cut surface, although the response mechanism has not been fully investigated.

In the jet upward deflection zone, the cutting process is considered as being controlled by erosive wear at large particle attack angles. This process is associated with jet upward deflection which increases the local rate of change of momentum. This zone is responsible for the raggedness of the cut at the bottom of the kerf and occurs only when the material is thick enough to prevent complete penetration.

The kerf geometry of a through cut generated by abrasive waterjets may be described as in Fig. 1. It is characterized by a small rounded corner at the top edge due to the plastic deformation of material caused by jet bombardment. As the kerf is wider at the top than at the bottom due to the decrease in water pressure, a taper is produced. In addition, the plastically deformed material rolls over at the bottom of the kerf forming burrs at the jet exit when cutting ductile materials.

Hashish and du Plassis [21] have proposed a model for jet spreading profile and strength zones, as shown in Fig. 2, in a study of the effect of standoff distance between the nozzle and workpiece. Hashish [18] later used this model to explain the kerf characteristics in abrasive waterjet cutting. These authors as well as Chen *et al.* [22] believed that the particle velocity at any cross-section of the jet should vary from zero at the nozzle wall to a maximum at the jet centre. This velocity distribution corresponds to an energy or strength distribution in the jet. The inner contoured regions of the jet, as shown in Fig. 2, which have higher velocities and are convergent, can result in tapered cuts on the material. The kerf width is dependent on the effective width (or diameter) of the jet, which in turn depends on the jet strength in that zone and the target material.

The primary interests in sheet steel processing are the kerf shape (kerf width and kerf taper) and kerf quality (cut surface roughness) as well as burrs which may be formed at the jet exit. These characteristics will be considered in the present study.

3. EXPERIMENTAL WORK

The experiment was conducted on a Flow Systems International Waterjet Cutter, equipped with a model 20X dual intensifier high output pump (380 MPa) and a five axis robot positioning system, to cut 80 mm long slots on 300×300 mm test specimens of 1 mm thick. The specimens were Zincalume G300 (hot-dipped aluminium/zinc alloy coated structural steel with a spangled surface) supplied by BHP Steels Pty. Ltd.. The coating thickness was about 0.021 to 0.025 mm on each side. The chemical composition of the substrate (structural steel) was 0.04-0.07% C, 0.01-0.02% P, 0.20-0.30% Mn, 0.01-0.02% S, 0.01-0.02% Si and 0.30-0.50% Al, with a yield strength of 330-390 MPa and a hardness of 55-65 HR30T. Some representative cuts were examined with an ‘Olympus’ stereo optical microscope for their quality and a JEOL (JSM-35CF) scanning electron microscope for the cutting mechanism. The kerf geometry (top and bottom kerf widths) was measured using a ‘Carl Zeiss’ universal optical measuring microscope. Three measurements were taken for each cut at the segment away from the ends of the slots to eliminate any effect of the cutting process at the jet entry and exit, and the average reading was taken as the geometrical value. The measurement of surface roughness, centre-line average R_a , was taken at the middle of the cut surface using a “Surtronic 3” stylus surface measuring facility with a cut-off length of 2.5 mm and a total length of 12.5 mm.

Although AWJ cutting involves a large number of variables, as noted by Hashish [4], and virtually all these variables affect the cutting results (cut depth, kerf width and kerf quality), only four major and easy-to-adjust dynamic variables as identified in the early work [4, 9] were considered in the present study. These included water pressure, nozzle traverse speed, abrasive flow rate and the standoff distance between the nozzle and the workpiece. The water pressure and abrasive flow rate were selected according to the common range of applications, shop floor practice and equipment limitations. In selecting the standoff distance, consideration was given to steel sheet bending and to avoiding contact between the nozzle and the workpiece. The approach to selecting the appropriate levels of traverse speed was such that at the predetermined maximum standoff distance, minimum abrasive flow rate and minimum water pressure, the traverse speed was adjusted for a through cut while at its maximum possible rate. Lesser traverse speeds were then selected at an appropriate spacing. It was felt that this approach would ensure that all the combinations of parameters selected would produce through cuts for evaluation. It should be mentioned that higher traverse speeds for through cut may be possible at the high level of settings for abrasive mass flow rate and water pressure and the low level of standoff distance used in the present study; the traverse speeds selected in this experiment were to ensure that through cuts could be achieved in all tests for comparison purpose. The optimum combination of the parameters for good quality through cuts will be discussed later in the paper.

Thus, three levels of waterjet pressure (240, 290 and 340 MPa), three levels of traverse speed (400, 600 and 800 mm/min), three levels of abrasive flow rate (0.4, 0.5 and 0.6 kg/min) and three levels of standoff distances (2, 3 and 4 mm) were tested using a single jet impact angle of 90°, i.e. the nozzle is normal to the workpiece surface. The other parameters which were kept constant included the orifice diameter (0.41 mm), the mixing tube diameter (1.27 mm), the length of mixing tube (88.9 mm), the nozzle diameter (1.02 mm), the nozzle length (76.2 mm), and the abrasive which was 80 mesh almandite garnet sand. Consequently, a total of 81 cuts (slits) were undertaken in this three-level four-factor full factorial designed experiment.

During the course of the experiments, care was taken to ensure that the wear of the nozzle did not have a large effect on the kerf geometry and quality. Frequent checks were made of the wear, when it became significant, the nozzle was replaced. In addition, some tests were replicated for cuts which were made directly on the top of the supporting bars and, hence, showed different characteristics.

4. VISUALISATION AND SCANNING ELECTRON MICROSCOPY STUDY

Observations of all the cuts revealed that AWJ produced clean slits of higher quality than those produced by CO₂ laser beam [1]. Kerf geometry was as shown in Fig. 1. Two types of burrs were observed, hard burrs and loose hair line burrs. Hard burrs were found at the jet exit side where the material attached firmly around the bottom cut edges, a secondary process was required to remove these. Loose hair line burrs were attached to the cut edges on both the jet exit side (bottom) and the jet entry side (top). These occurred due to peeling off of the hot dipped Aluminum/Zinc alloy coatings and were easily removed.

Some representative cuts were examined under an “Olympus” stereo optical microscope to evaluate the microscopic feature of the waterjet machined surfaces. The cut surfaces were of good finish although striations existed at the lower portion of some of the cuts. No microcracking was observed in any of the surfaces, nor was there any heat affected zone although this was anticipated. While there were a small number of abrasive particles embedded in the cut surfaces, as can be noticed in Fig. 3, they were readily removable using compressed air. Therefore, it may be stated that AWJ cutting is a viable and effective technology for metallic coated sheet steel processing with good quality and commercially acceptable productivity.

To study the cutting process and additional features of the machined surface, a scanning electron microscopy (SEM) analysis was conducted on a JEOL scanning electron microscope for some selected samples. An overall view for the cutting surfaces was taken at a magnification of 66X and then more enlarged views at 440X magnification were taken at different locations of interest to study the cutting process. When examining the morphology of the cutting front, the cutting action as a result of the impingement of individual abrasive particles was evident, as shown in Fig. 3. More detailed examination of SEM micrographs identified three distinct regions of the cut surface for further analysis, i.e. a top surface damaged region, a middle cutting region and a bottom exit region.

A small damaged region was formed by the initial jet bombardment where an indentation was produced on the edges of the top kerf by the waterjet and more grain facets were exposed in this area, as evidenced by the white band on the left hand side of Fig. 3(a). Below this, cutting marks can be seen. This may have been due to the two erosion stages (cutting wear and deformation wear) as proposed by other workers [4,23] for ductile material cutting. It is evident that the cutting at the upper portion was mainly by intergranular cracking where the material grains were pushed out by the abrasive particles and the plastic deformation in this region was not significant. This phenomenon can be seen on the left half of Figs. (a) and (c). In the middle cutting region, ploughing and scratching marks were observed, as shown from the middle region towards the right in Figs. (a) and (c) and the left half of Figs. (b) and (d), the interference of a particle and the work material being clearly visible in Fig. (d). This suggests that micromachining (cutting wear) and plastic deformation (deformation wear) are the dominant material removal mechanisms in this region. The degree of plastic deformation increases from the top to the bottom of the machined surfaces. At the lower portion, the so-called deformation wear becomes apparent and the abrasives push the material to deform until it is removed, as indicated on the right half of Fig. 3(b). Striations can be noticed on some selected samples at lower pressure and higher traverse

speed, where the grooving direction demonstrates the abrasive particles impacting at glancing angles to the eroded surface. However, the striation patterns were hardly discernible for the other samples, indicating that the cutting wear was dominant.

At the exit region, the cut surface shows relatively irregular pattern and the material is heavily deformed. This can be seen on the right hand side of Fig. (b) close to the edge of the photograph. The deformed material was not removed by the incomplete cutting actions but rolled over to form burrs at the bottom of the kerf.

Consequently, the cutting action for thin steels under abrasive waterjets may be considered as a result of the impingement of individual particles on the material. Micromachining and plastic deformation are the dominant processes. Burr formation is attributed to the incomplete cutting action of the particles and the rollover of the non-removed chips. In addition, striations or wavinesses may be formed for cutting with lower water pressure and higher traverse speed.

5. KERF CHARACTERISTICS

5.1 Effect of process parameters on kerf geometry

Kerf geometry is a characteristic of major interest in abrasive waterjet cutting. As discussed earlier, abrasive waterjets generally open a tapered slot with the top being wider than the bottom, as shown in Fig. 1, where the kerf taper is defined as a half of the kerf width variation per millimeter of depth of cut (or penetration).

Figs. 4 to 6 show some typical and representative trends and relationships between kerf geometry (top and bottom kerf widths and kerf taper) and the process parameters. It can be noticed from Fig. 4 that both the top and bottom kerf widths appear to increase with the water pressure. This may be expected as higher water pressure should result in greater jet kinetic energy and open a wider slot on the workpiece. It is interesting to note that water pressure exhibits a reduced effect on the top kerf width when it is increased from 290 MPa to 340 MPa. This is consistent with earlier findings [24, 25], i.e. abrasive waterjets become less effective at pressures above a threshold value depending on the other process parameters. The kerf taper in Fig. 4 shows somewhat similar trend as the top kerf. Since the bottom kerf width increases steadily with the water pressure, a decreased kerf taper is associated with the water pressure of 340 MPa where the width of top kerf shows flattening (or even decreasing).

The effect of standoff distance on the top kerf width, bottom kerf width and kerf taper is shown in Fig. 5. It can be seen that the top and bottom kerf widths increase with an increase in the standoff distance although the rate of increase for the bottom kerf width is smaller. This may be a result of jet divergence. Since the jet is losing its kinetic energy as it penetrates into the work material, the outer rim of the diverged jet does not take effect as it approaches the lower part of the kerf. As such, the standoff distance has a lesser effect on the bottom kerf width than the top. As a consequence of this effect, kerf taper is increasing with the standoff distance, as shown in Fig. 5.

Fig. 6 shows the effect of traverse speed on the kerf geometry, where the traverse speed exhibits a negative effect on both the top and bottom kerf widths, while the kerf taper appears to increase with the traverse speed. The negative effect of traverse speed on the kerf width is due to the fact that a faster passing of abrasive waterjet allows fewer particles to strike on the target material and hence generates a narrower slot. The increasing trend of the kerf taper is the result of the more rapidly decreasing kerf width at the bottom than at the top as the traverse speed increases.

The effect of abrasive flow rate on the kerf geometry can be noticed from Figs. 4 to 6. Within the range of abrasive flow rates tested, there is no clear trend of the kerf width with respect to the abrasive flow rate. In some cases, higher flow rate produces narrower kerf, as evidenced in the figures. This may be attributed to the fact that higher abrasive flow rate results in increased interference between particles, which reduces the effective number of impacts, alters favorable angles of attack and reduces impact velocities [4].

5.2 Effect of process parameters on surface roughness

Surface roughness and striation are the major factors in assessing kerf quality in AWJ cutting. While surface finish is a common phenomenon in all machining, striation or waviness is a special feature of cuts with beam cutting technology, such as AWJ cutting. It is formed when the ratio between the available energy of the beam and the required energy of the destruction becomes comparatively small [22]. In AWJ cutting, the cutting power of the jet decreases as it penetrates into the workpiece and striations are formed at the lower portion of the cut surface. As striation does not appear to be a common feature of the cut surface for thin sheet steels under abrasive waterjets, as noticed in the present study, only surface roughness as assessed by the centre-line average R_a was used in evaluating the kerf quality. Fig. 7 shows some typical trends of the surface roughness with respect to the traverse speed and abrasive flow rate while Table 1 gives the statistical data indicating the effect of water pressure and standoff distance.

From the experimental results, an increase in the traverse speed causes a constant increase in the surface roughness, as shown in Fig. 7. This may be anticipated as increasing the traverse speed allows less overlap machining action and fewer abrasive particles to impinge the surface, increasing the roughness of the surface. It can also be noticed from Fig. 7 that the surface roughness decreases with an increase in the abrasive flow rate. This may be attributed to the increased number of abrasive particles impinging the surface, as for the case of lower traverse speed.

It can be found from Table 1 that the surface roughness does not change linearly with the water pressure. It decreases initially with an increase in the water pressure, as indicated by the averages and ranges of the data for the water pressures of 240 MPa and 290 MPa. With a further increase in the water pressure, the surface roughness increases dramatically with the water pressure. For instance, when the water pressure increases from 290 to 340 MPa the average surface roughness increases by 24.2%, 14.4% and 35.3%, respectively, for the standoff distance of 2, 3 and 4 mm. This trend may be explained by the strength zones in a waterjet proposed by Hashish and du Plessis [21] and illustrated in Fig. 2. With the increase of the water pressure, the effective jet width (diameter) increases. As a consequence, the overlapping of a larger effective jet produces a wider kerf as well as a smoother surface than a smaller jet. As the pressure further increases, the outer rim of the diverged jet will gain enough energy for cutting the material which tends to increase the irregularity and roughness of the surface.

Increasing the standoff distance between the nozzle and workpiece resulted in a steady increase in the surface roughness, as evidenced in Table 1. This may be due to the fact that the waterjet diverges when spreading out from the mixing tube and this divergence results in not only wider kerf but also rougher surface.

5.3 Effect of process parameters on burr formation

As the loose hair line burrs can be easily removed, the main interest in this study was the hard burrs, and the burr height (Fig. 1) was used in the analysis. Due to the irregularity of the burrs

and the difficulty in measurement, the measured burr heights were grouped as categorical (or qualitative) values based on the threshold values given in Table 2.

Table 3 summarizes the number of burrs in each category under different cutting conditions. If the average value of the burr height in each category is used as a weighting factor to all the burrs in that category, e.g. 0.01 for category ‘burrless’, with 0.15 for the “very high” category, the average height (or weighted average) for different cutting conditions can be obtained to facilitate the analysis. This is given in the last column. It can be seen from the table that the majority of the slots with high and very high burrs are associated with the water pressure of 240 MPa. This is probably due to the deformation wear at the low water pressure, which resulted in the material to roll over at the bottom of the kerf.

From Table 3, the burr height steadily decreases with a decrease in the traverse speed. This is because slower traverse rate allows more thorough cutting and lower burrs to be formed. Increasing the standoff distance resulted in an increase in the burr height. This may be attributed to the jet power reduction as it flows away from the nozzle, resulting in high burrs due to the material deformation and roll over at low water pressure as mentioned above. Based on the average burr heights in the table, the effect of abrasive flow rate on burr formation is not evident.

5.4 Overall kerf characteristics and parameter selection consideration

In order to evaluate the overall characteristics of the kerfs generated on surface coated sheet steels under abrasive waterjets, the above analyses and trends are summarized and given in Table 4, where the ‘increase’ and ‘decrease’ indicate the increasing and decreasing trends of the quantities, respectively, with an increase in each of the four variables, while the surface roughness exhibits a minimum turning point corresponding to an optimum water pressure. It appears that an increase in the standoff distance will result in an increase in all the four quantities and therefore it should be selected as small as possible. Within the range considered, the abrasive flow rate does not show significant effect on the kerf geometry and burr height but a slight effect on the surface roughness. As such, unless the surface finish is a major concern, a small abrasive flow rate may be used from the economic point of view. Increasing traverse speed will result in increased surface roughness, kerf taper and burr height, but decreased kerf width. Nevertheless, traverse speed is directly proportional to the productivity and should be selected as high as possible without compromising the kerf quality, i.e. in the vicinity of 800 mm/min.

By contrast, the effect of water pressure on the kerf characteristics is interesting. While an increase in the water pressure will result in a constant increase in kerf width and a constant decrease in burr height, it does not affect the kerf taper significantly based on the analysis. Interestingly, there is a minimum point associated with the surface roughness as the water pressure varies. The optimum water pressure is dependent on the other process parameters and the work material used. In the present study, this optimum pressure is between 240 and 340 MPa, and 290 MPa would be a good approximation. In addition, the water pressure is found to affect only slightly the burr height in the high pressure range, as indicated by the average heights in Table 3. Thus, high water pressure in the vicinity of its optimum value should be selected. This selection will give good surface finish and low burr height and allow high traverse speed to be used while maintaining the desired kerf quality.

It may be noted that if the kerf width and kerf taper can be predicted, they may be compensated in the design and process planning stages and by controlling the nozzle angle in the machine. Likewise, knowing the surface roughness prior to cutting will enhance the likelihood of accomplishing the required surface finish. Thus, the establishment of empirical predictive models for the kerf characteristics will be considered below.

5.5 Empirical models for kerf characteristics

A regression analysis has been carried out to establish empirical models relating the kerf characteristics to the process variables. Since burr formation was treated as a categorical value, empirical equations were obtained for top kerf width, kerf taper and surface roughness in terms of the four major process variables.

An outlier analysis showed that except for the five cuts which were made directly on the top of the supporting bar in the machine and were excluded from all the analyses, no outliers were detected. The regression procedure was conducted using an SPSS package. Five different possible models were tested for each of the three quantities at a confidence interval of 95%. They were straight line model, exponential model, power model, logarithmic model and quadratic model. Examining the coefficients of determination (R^2) showed that the quadratic model gave the highest R^2 values of 93%, 92% and 88% for the top kerf width, kerf taper and surface roughness, respectively. Thus, further analysis was made on the quadratic model with interactions.

For a four factor experiment, 15 estimated parameters are needed to fit a quadratic model and the resulting model is likely to be too complicated for practical use. Therefore, the 'backward elimination' procedure available in the SPSS package was used and the final simplified models for the top kerf width, kerf taper and surface roughness (centre-line average) were obtained and are given as follows:

Top kerf width:

$$W_t = -1.554 + 0.019P + (4.33S_d + 11.4V S_d - 0.01785V P + 4.33S_d P - 0.3216P^2)10^{-4} \quad (1)$$

Kerf taper:

$$T_a = -1.067 + 0.008P - 0.212F_r - (0.0789V P + 3.887F_r S_d + 1.906V S_d - 1.363P^2 + 0.02016V^2)10^{-5} \quad (2)$$

Roughness (centre-line average):

$$R_a = 34.506 - 0.221P + (4V - 0.9242V S_d + 5S_d P - F_r S_d + 0.3717P^2)10^{-3} \quad (3)$$

where W_t = top kerf width (mm)

T_a = kerf taper (mm/mm)

R_a = centre-line average (μm)

P = water pressure (MPa)

V = traverse speed (mm/min)

S_d = standoff distance (mm)

F_r = abrasive flow rate (kg/min)

These equations are applicable for the test conditions and the ranges of the variables specified in the section on experimental work. From equations (1) and (2), the bottom kerf width may be obtained. The R^2 values for the three simplified equations are respectively 91%, 89% and 86%. F-tests have been conducted and showed strong evidence of the utility of the three models. Similarly, T-tests have indicated that there are strong evidence of linear relationships between the response variables (top kerf width, kerf taper and surface roughness) and all the individual explanatory parameters in the final equations. In addition, comparisons between the model predicted and experimental results have shown that the empirical models correlate very well with

the experimental data, as shown in Fig. 8. Consequently, the established empirical equations can be used to estimate kerf characteristics for the conditions within the ranges of this study.

6. CONCLUSIONS

A study of AWJ cutting of metallic coated sheet steels has been presented. It has been shown that AWJ cutting is a viable and effective technology for processing metallic coated sheet steels with good kerf quality and commercially acceptable productivity. Micromachining and plastic deformation have been found to be the dominant cutting processes in sheet steel processing from the SEM analysis. Plausible kerf characteristics as assessed by kerf geometry, surface roughness and burr formation in terms of process parameters have been amply discussed from which recommendations have been made on the selection of the process variables. The regression analysis has provided empirical models for the prediction and optimization of AWJ cutting performance for the material under consideration.

Acknowledgments: The authors wish to thank Mr. John Gatt, Queensland Manufacturing Institute (QMI), for his assistance in the experimental work. Thanks are also due to Mr. Jim S.H. Hoe for his help in data acquisition and regression analysis.

REFERENCES

- [1] P.V.S. GUDIMETLA, Laser cutting of metallic coated sheet steels, *M. Eng. Sc. Thesis*, Queensland University of Technology (1995).
- [2] C.A. VAN LUTTERVELT, On the selection of manufacturing methods illustrated by an overview of separation techniques for sheet materials, *Annals of CIRP*, **38**(2), 587-607 (1989).
- [3] N.S. GUO, G. LOUIS and G. MEIER, Surface structure and kerf geometry in abrasive waterjet cutting: Formation and optimization, *7th American Waterjet Conf.*, Seattle, Washington, USA, 1-25 (1993).
- [4] M. HASHISH, A modeling study of metal cutting with abrasive waterjets, *J. Eng. Mater. Technol.*, **106**, 221-228 (1984).
- [5] M. HASHISH, A model for abrasive waterjet performance optimization, *J. Eng. Mater. Technol.*, **111**, 154-162 (1989).
- [6] S. MATSUI, H. MATSUMURA, Y. IKEMOTO, K. TSUJITA and H. SHIMIZU, High precision cutting methods for metallic materials by abrasive waterjet, *Proc. 10th Int. Symp. on Jet Cutting Technology*, Cranfield, UK, 263-278 (1990).
- [7] M. HASHISH, On the modeling surface waviness produced by abrasive waterjets, *Proc. 11th Int. Symp. on Jet Cutting Technology*, Dordrecht, The Netherlands, 17-34 (1992).
- [8] I. FINNIE, J. WOLAK and Y. KABIL, Erosion of metals by solid particles, *J. Materials*, **2**, 682-700 (1967).
- [9] L. CHEN, E. SIORES and W.C.K. WONG, Kerf characteristics in abrasive waterjet cutting of ceramic materials, *Int. J. Mach. Tools Manuf.*, **36**(11), 1201-1206 (1996).
- [10] E. SIORES, W.C.K. WONG, L. CHEN and J.G. WAGER, Enhancing abrasive waterjet cutting of ceramics by head oscillation techniques, *Annals of CIRP*, **45**(1), 215-218 (1996).
- [11] J. ZENG and T.J. KIM, Development of an abrasive waterjet kerf cutting model for brittle materials, *Proc. 11th Int. Symp. on Jet Cutting Technology*, Scotland, 483-503 (1992).
- [12] R.J. WILKINS and E.E. GRAHAM, An Erosion Model for Waterjet Cutting, *J. Eng. Ind.*, **115**, 57-61 (1993).
- [13] D.K.M. TAN, A model for the surface finish in abrasive-waterjet cutting, *Proc. 8th Int. Symp. on Jet Cutting Technology*, Cranfield, UK, 309-313 (1986).

- [14] J. CHAO, E.S. GESKIN and Y. CHUNG, Investigation of the dynamics of surface topography formation during abrasive waterjet cutting, *Proc. 11th Int. Symp. on Jet Cutting Technology*, Dordrecht, The Netherlands, 593-603 (1992).
- [15] R. KOVACEVIC, Surface texture in abrasive waterjet cutting, *J. Manuf. Systems*, **10**(1), 32-40 (1991).
- [16] W. KOENIG, Machining of fibre reinforced plastics, *Annals of CIRP*, **34**/2, 537-548 (1985).
- [17] J. WANG and W.C.K. WONG, Abrasive waterjet machining of polymer matrix composites - cutting performance, erosive process and predictive models, to appear in the International Journal of Advanced Manufacturing Technology.
- [18] M. HASHISH, Characteristics of surfaces machined with abrasive waterjets, *J. Eng. Mater. Technol.*, **113**, 354-362 (1991).
- [19] J.G.A. BITTER, A study of erosion phenomena: Part I, *Wear*, **6**, 5-21 (1963).
- [20] I. FINNIE, The mechanism of erosion of ductile metals, *Proc. 3rd National Congress of Applied Mechanics*, ASME, 527-532 (1958).
- [21] M. HASHISH and M.P. DU PLESSIS, Prediction equations relating high velocity jet cutting performance to standoff distance and multipasses, *J. Eng. Ind.*, **101**, 311-318 (1979).
- [22] L. CHEN, E. SIORES and W.C.K. WONG, High-pressure abrasive waterjet erosion process, *Proc. Australasian Conf. Manuf.*, Seoul, Korea, 642-647 (1996).
- [23] G.P. TILLY, A two stage mechanism of ductile erosion, *Wear*, **23**, 87-96 (1973).
- [24] M. HASHISH, Pressure effects in abrasive waterjet machining, *J. Eng. Mater. Technol.*, **111**, 221-228 (1989).
- [25] K. FABER and H. OWEINAH, Influence of process parameters on blasting performance with the abrasive jet, *Proc. 10th Int. Symp. on Jet Technology*, The Netherlands, 193-206 (1990).

List of captions for tables

Table 1. The effect of standoff distance and waterjet pressure on surface roughness R_a (μm).

Table 2. Categories of burr height.

Table 3. The effect of process parameters on burr formation.

Table 4. Kerf characteristics in terms of process parameters.

List of captions for figures

Fig. 1. Schematic and definition of kerf geometry.

Fig. 2. Relative strength zones in a waterjet [21].

Fig. 3. Scanning electron micrographs. (a) and (c): views close to the top kerf; (b) and (d): views close to the bottom kerf.

Cutting conditions: views (a) and (b): water pressure = 340 MPa, traverse speed = 800 mm/min, standoff distance = 2 mm, and abrasive flow rate = 0.5 kg/min; views (c) and (d): water pressure = 290 MPa, traverse speed = 400 mm/min, standoff distance = 3 mm, and abrasive flow rate = 0.4 kg/min.

Fig. 4. The effect of water pressure on kerf geometry (traverse speed = 800 mm/min, standoff distance = 2 mm).

Fig. 5. The effect of standoff distance on kerf geometry (water pressure = 340 MPa, traverse speed = 600 mm/min).

Fig. 6. The effect of traverse speed on kerf geometry (water pressure = 340 Mpa, standoff distance = 3 mm).

Fig. 7. The effect of traverse speed on surface roughness (centre-line average).

Fig. 8. Experimental vs. predicted values of kerf width, kerf taper and surface roughness (line drawings indicate the ideal cases).

TABLE 1. THE EFFECT OF STANDOFF DISTANCE AND WATERJET PRESSURE ON SURFACE ROUGHNESS R_a (μm).

Waterjet pressure	Standoff distance					
	2 mm		3 mm		4 mm	
	R_a range	average R_a	R_a range	average R_a	R_a range	average R_a
240 MPa	4.86-6.70	5.81	5.06-7.22	6.18	5.09-7.14	6.29
290 MPa	4.80-5.94	5.30	5.28-6.61	5.91	5.36-6.72	5.92
340 MPa	5.80-7.70	6.58	5.83-7.50	6.76	7.39-8.75	8.01

TABLE 2. CATEGORIES OF BURR HEIGHT.

Burr category	Burr height (mm)
Burrless	0-0.02
Low burr	0.02-0.05
Median burr	0.05-0.08
High burr	0.08-0.12
Very high burr	>0.12

TABLE 3. THE EFFECT OF PROCESS PARAMETERS ON BURR FORMATION.

		Number of burrs					Average height (mm)
		Burrless	Low burr	Med. burr	High burr	V/high burr	
Water pressure (MPa)	240	2	0	3	14	8	0.104
	290	2	7	14	2	2	0.062
	340	2	5	17	3	0	0.059
Traverse Speed (mm/min)	400	4	6	11	6	0	0.058
	600	4	4	11	4	4	0.070
	800	1	2	12	8	4	0.084
Standoff distance (mm)	2	4	4	11	7	1	0.065
	3	3	6	11	3	4	0.069
	4	2	2	12	8	3	0.079
Abrasive flow rate (kg/min)	0.4	3	4	11	7	2	0.070
	0.5	3	5	8	8	3	0.073
	0.6	3	3	14	4	3	0.070

TABLE 4. KERF CHARACTERISTICS IN TERMS OF PROCESS PARAMETERS.

	Water pressure	Standoff distance	Abrasive flow rate	Traverse speed
Kerf width	increase	increase	not significant	decrease
Kerf taper	not significant	increase	not significant	increase
Surface roughness	with a minimum	increase	decrease	increase
Burr height	decrease	increase	not significant	increase

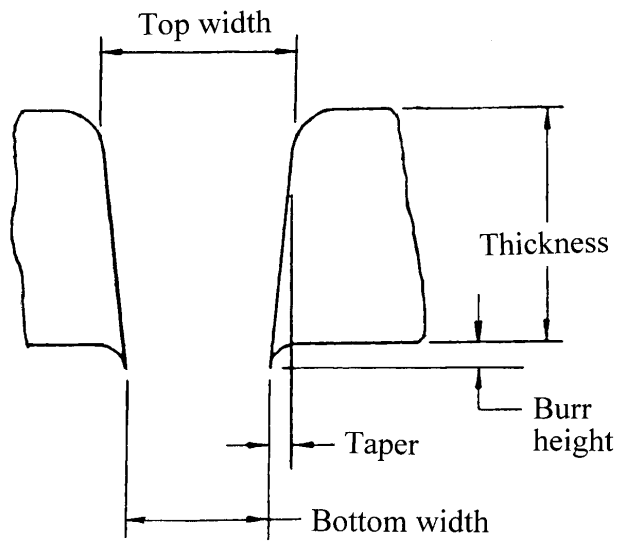


FIG. 1. Schematic and definition of kerf geometry.

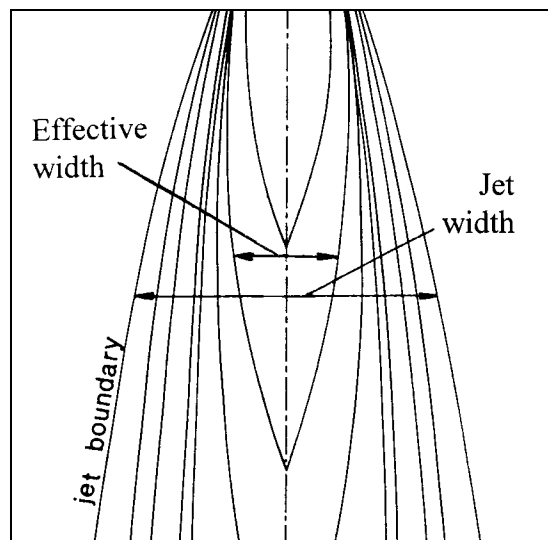
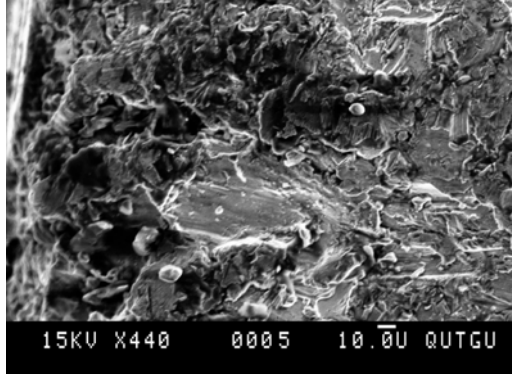


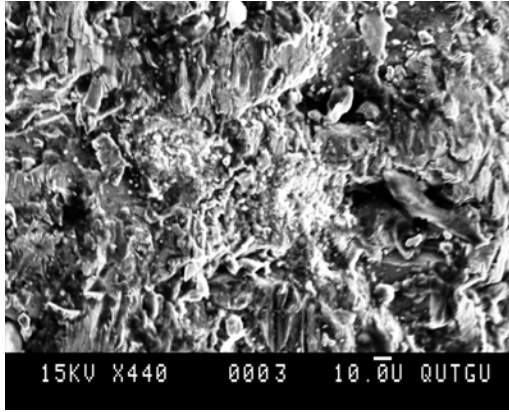
FIG. 2. Relative strength zones in a waterjet [21].



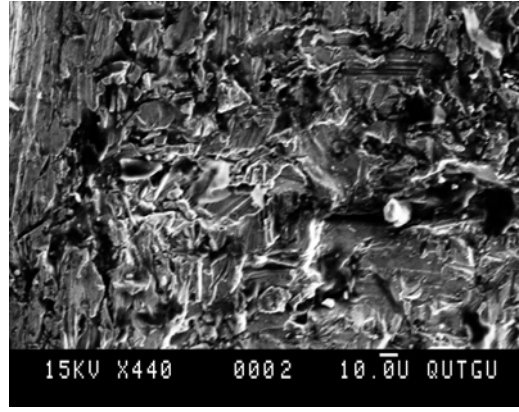
(a)



(b)



(c)



(d)

[Initial jet (cutting) direction: →]

FIG. 3. Scanning electron micrographs. (a) and (c): views close to the top kerf; (b) and (d): views close to the bottom kerf.

Cutting conditions: views (a) and (b): water pressure = 340 MPa, traverse speed = 800 mm/min, standoff distance = 2 mm, and abrasive flow rate = 0.5 kg/min; views (c) and (d): water pressure = 290 MPa, traverse speed = 400 mm/min, standoff distance = 3 mm, and abrasive flow rate = 0.4 kg/min.

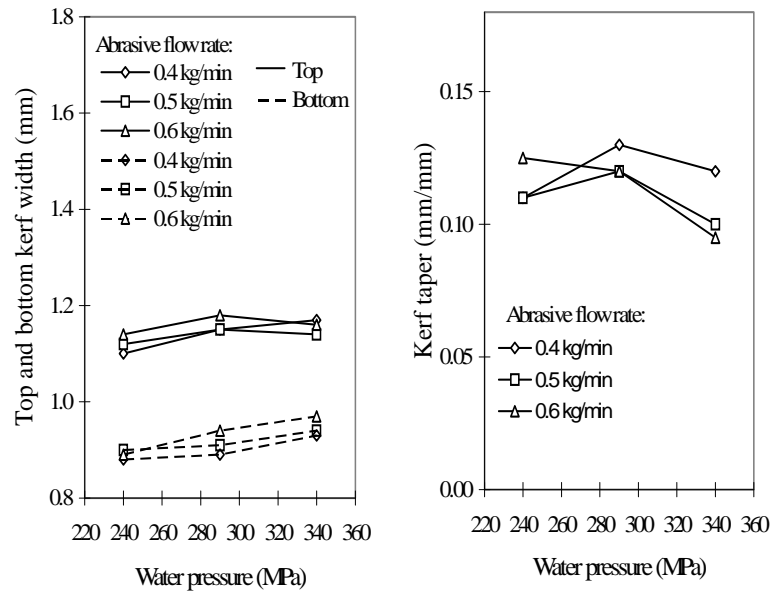


FIG. 4. The effect of water pressure on kerf geometry (Traverse speed = 800 mm/min, standoff distance = 2 mm).

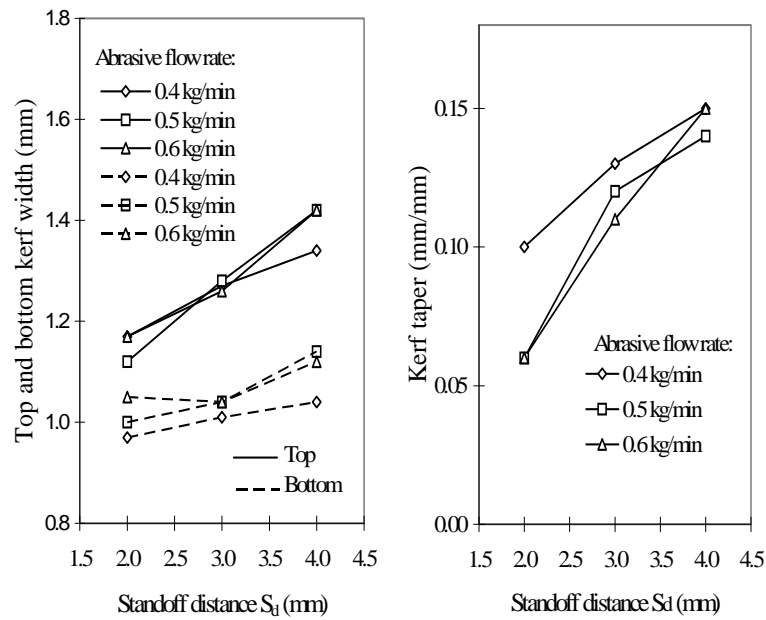


FIG. 5. The effect of standoff distance on kerf geometry (water pressure = 340 MPa, traverse speed = 600 mm/min).

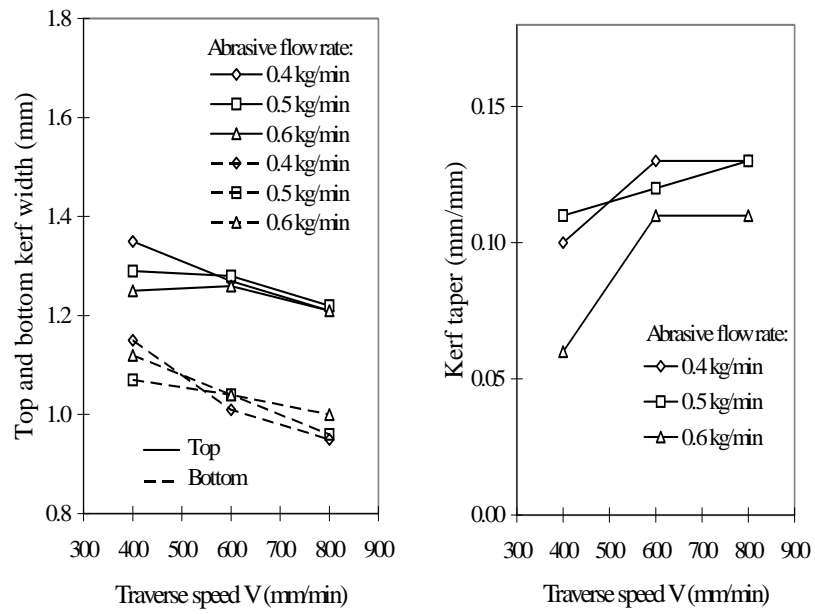


FIG. 6. The effect of traverse speed on kerf geometry (water pressure = 340 Mpa, standoff distance = 3 mm).

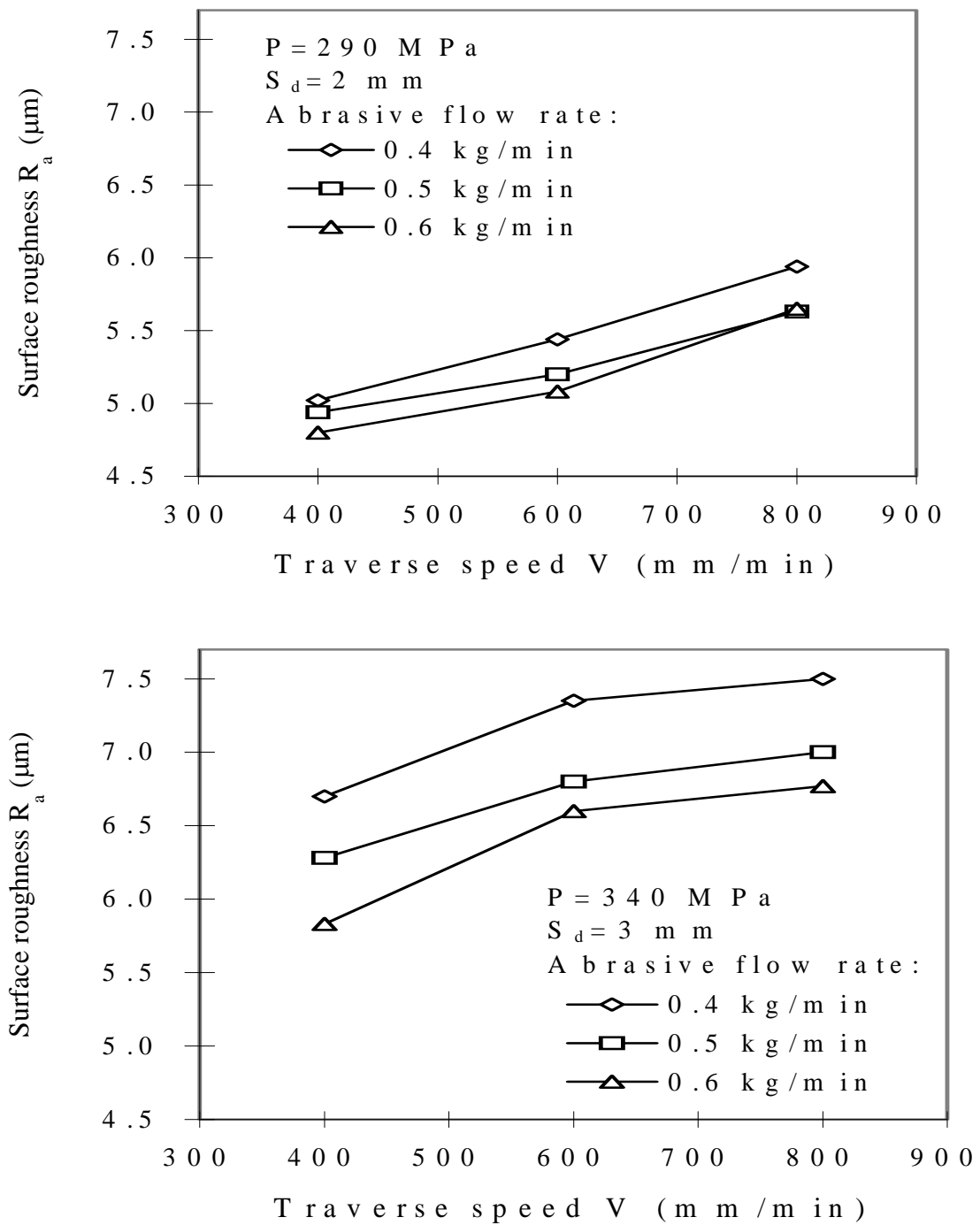


FIG. 7. The effect of traverse speed on surface roughness (centre-line average).

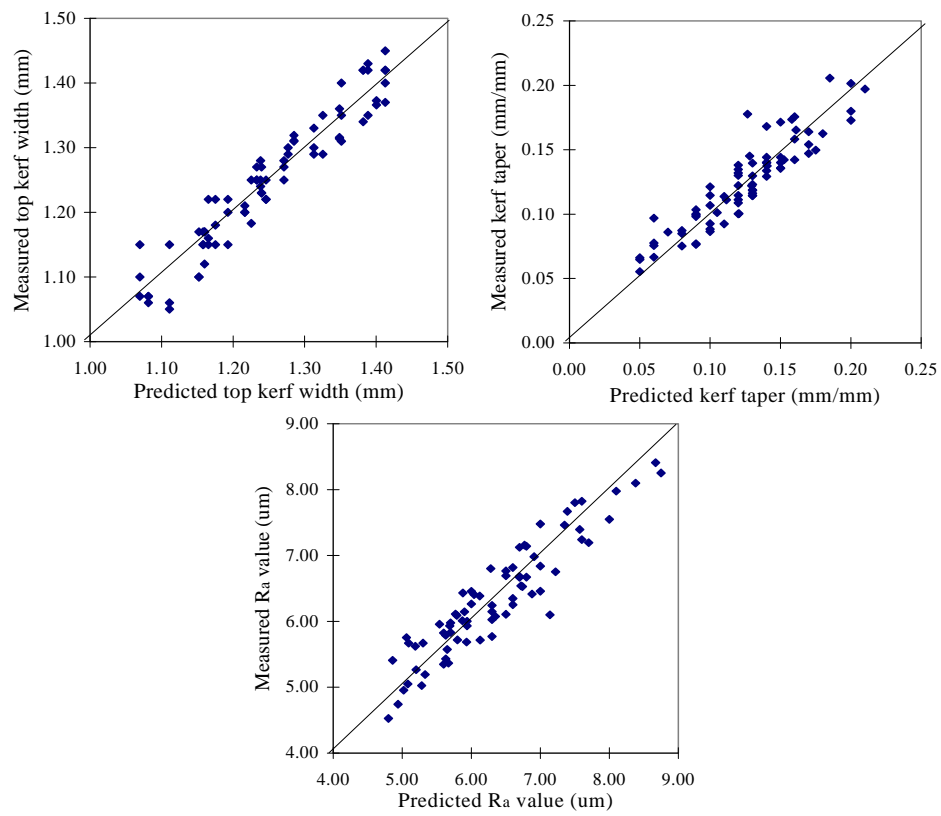


FIG. 8. Experimental vs. predicted values of kerf width, kerf taper and surface roughness (line drawings indicate the ideal cases).